International Journal of ISSI, Vol.3 (2006), No. 1, pp. 26-32

Simulation of Temperature Distribution in Hot Strip over Transfer Table

A. Saboonchi* and N. Mansouri
Department of Mechanical Engineering, Isfahan University of Technology, Isfahan, Iran
Received March 11, 2006; Accepted November 19, 2006

Abstract
Transfer table is an essential stage between roughing and finishing rolling stands in a hot-strip rolling mill. High temperature and long time that strip is exposed to air at this stage cause a considerable heat loss that accounts for uneven temperature distribution, non-uniform surfaces, reduced product quality and increased production costs. Using thermal shields on the transfer table is considered an efficient means of reducing energy consumption and of improving product quality. In this paper, temperature distribution and heat loss from the strip is investigated while passing through transfer table in the hot-rolling at Mobarakeh Steel Complex (MSC), Isfahan, Iran. Three cases are considered; namely, in the absence of thermal shield, in the presence of thermal shield, and with both thermal shield and heat source. The results obtained from the numerical solution indicate that the case with both thermal shield and heat source on the transfer table has the most favorable effect on reducing heat losses and even temperature distribution in the strip.

Keywords: Hot-Strip Rolling, Transfer table, Strip, Temperature distribution, Thermal sield.

Symbols

Nu	Nusselt number	ρ	Density (Kg/m^3)
Re	Reynolds number	c	Specific heat capacity ($J/Kg.K$)
Pr	Prandtl number	k	Thermal conductivity ($W/m.K$)
Gr	Grashhof number	T	Temperature (K)
Ra	Rayleigh number	σ	Stephan boultzman constant ($W/m^2.K^4$)
ξ	Buoyancy parameter	ε	Emmisivity factor
g	Acceleration gravity (m/s^2)	F	Configuration factor
β	Expansion coefficient ($1/K$)	h	Convection heat transfer coefficient ($W/m^2.K$)
ν	Kinematics viscosity (m^2/s)	A	Area (m^2)
L	Representative length (m)	P	Pressure (N/m^2)

Introduction

Modeling of hot-rolling process is undoubtedly an essential research endeavor to optimize steel rolling processes. Prediction of temperature distribution in the strip is of special importance as temperature is an important metallurgical parameter during the rolling process because properties and dimensions of steel greatly depend on the temperature distribution in the strip. Furthermore, prediction of the amount of strip temperature drop allows us to determine the required temperature of the strip leaving the preheating furnace. Obviously, this knowledge can lead to adoption of certain measures to reduce strip heat loss and thus, to reduce the preheating temperature.

* *Corresponding author:*
Tel:+98-311-3915221 Fax: +98-311-3912628
E-mail: ahmadsab@cc.iut.ac.ir
Address: Dept. of. Mechanical Enginerring, Isfahan University of Technology, Isfahan, 8415683111, IRAN

Due to the long distance between roughing and finishing stands and rather long time the strip is exposed to air, radiative heat loss from the strip is great. Some researchers have investigated various ways to reduce the rate of heat loss. One of the most common methods is the use of thermal shields.

Ginzburg[1)] developed the principles of computer simulation of rolling mills. His simulation resulted in optimized production conditions, improved product quality, and energy savings.

Ginzburg and Schmiedberg[2)] studied the main parameters involved in temperature variation during rolling process and methods of avoiding heat losses between roughing and finishing stands in order to determine optimized working conditions. According to them, the main parameters in changing temperature include temperature losses due to radiation and convection to the environment and rolls, conductive heat transfer to work rolls and water spray for oxide removal, and temperature gains due to friction and mechanical work of rolls. In addition, they ascribed great temperature changes of

hot strip along its transverse direction related to radiation at the edges.

Serajzadeh, Karimi, and Mucciardi[3] investigated temperature distribution in hot strip passing through hot rolling. They developed a finite element mathematical model to predict temperature distribution and metallurgical changes in the steel strip. In their model, a number of parameters were considered like deforming temperature, work roll temperature, rolling speed, and heat transfer coefficient between the metal and the work rolls. They also studied temperature distribution in work rolls of hot rolling[4]. They developed a finite element model and solved two-dimensional and transient heat transfer equations with time-dependent boundary conditions to predict temperature distribution in work rolls. In a similar study, Serajzadeh and Mucciardi[5] studied temperature distribution in work rolls.

Serajzadeh[6] investigated temperature distribution and phase changes in run-out table in hot rolling. In predicting cooling rate of low carbon steel, he used the finite element method and the Scheil-addivity rule.

Hosseini Beheshti[7] studied heat transfer in the strip while passing through transfer table in two cases, with and without thermal shield. To compute the heat loss from the strip, he studied the two-dimensional energy balance using a finite difference method. In this method, convective heat transfer from the top surface was assumed to be combined due to its high temperature. Furthermore, the conductive heat transfer inside the strip was assumed to be small, and because of geometrical complexity of the surface below the strip, all types of heat transfer from this surface were neglected.

Only one study has been conducted on simulating heat transfer of strip in hot rolling mill of Mobarakeh Steel Complex. However, this study did not consider the conductive heat transfer inside the strip nor did they consider heat transfer from the bottom surface.

In this study, temperature distribution in strip while passing through transfer table between last roughing shelf and first finishing shelf is predicted by considering radiation and convection from top, bottom and around it and also by considering of conduction inside it. This prediction is for the three cases of without thermal shield, with thermal shield, and with thermal shield and heat source. It should be mentioned that by the time this research was done, thermal shield hadn't been installed above transfer table in Mobarakeh Steel Complex, and there wasn't practical result for these cases.

Heat loss from the strip while passing through transfer table:

Heat release from strip passing through transfer table consists of two forms: convection and radiation. Due to convective heat transfer from strip surfaces and from upper surface of the thermal shield, the equations for free, forced, and combined convection have been used. Also, convection equations have been used related to isotherm plain due to low temperature discrepancies among points along the strip in each time step.

Convective heat transfer coefficients at bottom surface of strip are computed by using forced convection heat transfer equations. The local Nusselt number for forced flow is obtained from the analogical solution for laminar flow, and experimental results for turbulent flow. All characteristics are used in the film temperature, $T_f=(T_\infty+T)/2$.

$$Nu_x = 0.332\,\mathrm{Re}_x^{1/2}\,\mathrm{Pr}^{1/3} \quad 0.6 \le \mathrm{Pr} \le 50 \tag{1}$$

$$Nu_x = 0.0296\,\mathrm{Re}_x^{4/5}\,\mathrm{Pr}^{1/3} \quad 0.6 \le \mathrm{Pr} \le 50 \tag{2}$$

For the forced flow, the laminar to turbulent exchange point is assumed to take place at Reynolds Number 5×10^5.

Convective heat transfer coefficients at upper surface thermal shield are computed from the free convection heat transfer equations. The dimensionless Grashhof number in free flow is expressed as:

$$Gr_L = \frac{g\,\beta\,(T-T_\infty)\,L^3}{\nu^2} \tag{3}$$

Where $\beta=1/T_f$ is expansion coefficient, T is surface temperature, T_∞ is fluid temperature at a long distance, ν is kinematics viscosity, g is acceleration of gravity, and L is representative length which is the ratio of surface to environment.

Using empirical relations for common geometrical shapes, the mean Nusselt number will be obtained as follows:

$$\overline{Nu}_L = C\,Ra_L^n \tag{4}$$

Where Rayleigh number, Ra_L, is expressed as:

$$Ra_L = Gr_L\,\mathrm{Pr} \tag{5}$$

Incropra [8] found mean Nusselt number for a hot strip facing upward:

$$\begin{aligned} \overline{Nu}_L &= 0.54\,Ra_L^{1/4} && 10^4 \le \mathrm{Pr} \le 10^7 \\ \overline{Nu}_L &= 0.15\,Ra_L^{1/3} && 10^7 \le \mathrm{Pr} \le 10^{11} \end{aligned} \tag{6}$$

With regard to high temperature of the moving strip, convective heat transfer coefficients in the upper surface of the strip are computed from the combined convective heat transfer equations. Empirical results indicate that the combined local Nusselt number can be obtained from the following relation:

$$Nu^n = Nu_F^n \pm Nu_N^n \tag{7}$$

Where Nu_N and Nu_F are local Nusselt numbers in free and forced flows, respectively, and n is a constant. Positive sign designates agreeable and negative sign designates opposed flows. Defining $X = \dfrac{Nu_N}{Nu_F}$ and $Y = \dfrac{Nu}{Nu_F}$, we will have:

$$Y^n = 1 + X^n \tag{8}$$

Local Nusselt numbers for laminar flow in

forced and free flows is:

$$Nu_F = A(\mathrm{Pr})\,\mathrm{Re}_x^{1/2}$$
$$Nu_N = B(\mathrm{Pr})\,Gr_x^{1/2} \quad (9)$$

A(Pr) and *B(Pr)* are functions in terms of Prandtle number. Substituting Relation (9) in (8), we will have:

$$\frac{Nu\,\mathrm{Re}_x^{-1/2}}{A(\mathrm{Pr})} = \left[1 \pm \left(\frac{B(\mathrm{Pr})\,\xi^m}{A(\mathrm{Pr})}\right)^n\right]^{1/n} \quad (10)$$

Where $\xi = \frac{Gr}{\mathrm{Re}^{1/2m}}$ is buoyancy parameter, and m is a numerical constant which depends on kind of flow and heat boundary conditions in the net free flow. The above relation is presented for a moving plain[9]. For isothermal boundary conditions or constant rate of heat transfer, m = 0.2, n = 3, and values for *A(*Pr*) and B(*Pr*)* are computed from the following relation. All properties should be calculated in film temperature.

$$A(\mathrm{Pr}) = 1.886\,\mathrm{Pr}^{13/32} - 1.445\,\mathrm{Pr}^{1/3}$$
$$B(\mathrm{Pr}) = \frac{(\mathrm{Pr}/5)^{1/5}\,\mathrm{Pr}^{1/2}}{0.25 + 1.6\,\mathrm{Pr}^{1/2}} \quad (11)$$

Local Nusselt numbers in turbulent flow are given as follows for forced[10] and the free flows[11]:

(12)

$$Nu_F\,\mathrm{Re}_x^{-4/5} = 0.0287\mathrm{Pr}^{0.6} \qquad 0.5 \le \mathrm{Pr} \le 10, 5\times10^5 \le \mathrm{Re}_x \le 5\times10^6$$
$$Nu_N\,Gr_x^{-1/3} = 0.13\mathrm{Pr}^{1/3} \qquad Gr_x\,\mathrm{Pr} \ge 5\times10^8$$

Substituting (12) in (8) we will have:

$$\frac{Nu\,\mathrm{Re}_x^{-4/5}}{F(\mathrm{Pr})} = \left[1 \pm C\left(\frac{G(\mathrm{Pr})}{F(\mathrm{Pr})}\left(\frac{Gr_x}{\mathrm{Re}_x^{12/5}}\right)^{1/3}\right)^n\right]^{1/n} \quad (13)$$

Where n =3, C = 0.006, F(Pr) = 0.0287Pr$^{0.6}$, and G(Pr) = 0.13Pr$^{1/3}$. According to results from Hayashi[12], under these conditions, the laminar to turbulent transfer exchange occurs where $\frac{Gr_x}{\mathrm{Re}_x^{3/2}} = 192$.

The first step in computing radiative heat loss is to determine the radiative configuration factors. They have been calculated from Howell's results[13]. Configuration factors of an element in relation to rectangular plane and cylinder (rollers) were used in radiation calculation.

In the case which combustion occurs inside thermal shield, considerable amount of water vapor and carbon dioxide is formed. Therefore, assumption of transparent medium is not correct and it must be assumed that the medium has the capability of absorption and emission. Computation of gas radiation properties is complicated, Hottel[14] developed a simple method to compute emissivity coefficient of mixed gas. In this method, combustion equation should be written and partial pressures of water vapor P_w and carbon dioxide P_c are computed from it. By using P_w, P_c, and representative length L_e that is portion of volume to area, emissivity coefficients of water vapor, carbon dioxide, correction value $\Delta\varepsilon$, and coefficient values of water vapor C_w and carbon dioxide C_c can be obtained from related graphs. At last, emissivity coefficient of mixed gas can be calculated from following relation:

$$\varepsilon_g = C_w\,\varepsilon_w + C_c\,\varepsilon_c - \Delta\varepsilon \quad (14)$$

In this case, the absorption and emission coefficient of combustion gases have been computed on the basis of complete combustion of methane mixed with 10% additional air under atmospheric pressure.

(15)

$$CH_4 + 2.2(O_2 + 3.76N_2) \rightarrow Co_2 + 2H_20 + 0.2O_2 + 8.272\,N_2$$

Numerical solution

In the present study, heat loss has been computed for a strip 75,000 mm long, 1,000 mm wide, and 35 mm thick. These dimensions can be varied according to product type. A structured grid has been used in the solution. Given that the thickness is smaller in size than the other two dimensions, the solution has been accomplished along two directions. Because of the symmetry in the width of the strip, the problem has been solved over half of the slab.

Regarding the fact that the greatest heat is lost by radiation, radiative boundary condition for edges of the strip has been taken into consideration. For the middle half of the strip, symmetry boundary condition has been considered. An initial temperature of 1050 °C has been assumed for each element at the last stand in the roughing when it enters transfer table. This temperature is measured by MSC at hot rolling mill.

In the numerical simulation, an energy balance has been written for an arbitrary element of the strip with length Δx, width Δy, and thickness Δz. Heat transfer for each element consists of conduction with adjacent elements, radiation from the top and bottom of it to environment and to the carrier roll and thermal shield, and at last convective heat transfer from the top and bottom of the element to the environment.

The energy balance for an element in the case which there is no thermal shield will be parabolic as follows:

(16)

$$\frac{\partial T}{\partial t} = \frac{k}{\rho c}\left(\frac{\partial^2 T}{\partial x^2} + \frac{\partial^2 T}{\partial y^2}\right) - \frac{1}{\rho c\,\Delta z}\left[h_{up}(T - T_{up}) + h_{down}(T - T_{down})\right]$$
$$- \frac{\sigma\varepsilon}{\rho c\,\Delta z}\left[(T^4 - T_{up\infty}^4) + F_{e-roll}(T^4 - T_{roll}^4) + F_{e-down}(T^4 - T_{down\infty}^4)\right]$$

Where ρ, c, k, ε, and T are respectively density, specific heat capacity, thermal conductivity (which these parameters are calculated at element temperature), emissivity factor and temperature of the element, T_{up}, and T_{down} are ambient temperature around top and bottom of strip, $T_{up\infty}$, and $T_{down\infty}$ are

ambient temperature at a distance from top and bottom of strip, $F_{e\text{-}roll}$ and $F_{e\text{-}down}$ are the element configuration factor to carrier rollers and bottom environment and σ is Stephan Boultzman constant with value of 5.67×10^{-8}. Value for h_{up} was given from relation (13) and for h_{down} was given from relations (1) and (2).

In the case that there is thermal shield, energy balance for an element will be in the form of following equation:

$$\frac{\partial T}{\partial t}=\frac{k}{\rho c}\left(\frac{\partial^2 T}{\partial x^2}+\frac{\partial^2 T}{\partial y^2}\right)-\frac{1}{\rho c\Delta z}\left[h_{up}\left(T-(T+T_3)/2\right)+h_{down}(T-T_{down})\right] \quad (17)$$
$$-\frac{\sigma}{\rho c\Delta z}\left[\frac{(T^4-T_3^4)}{R}+F_{e-roll}\varepsilon(T^4-T_{roll}^4)+F_{e-down}\varepsilon(T^4-T_{down\infty}^4)+F_{e-up\infty}\varepsilon(T^4-T_{up\infty}^4)\right]$$

Where R is circuit equivalent radiation resistance

$$R=\frac{1-\varepsilon}{\varepsilon}+\frac{1}{F_{e-tun}}+\frac{1-\varepsilon_3}{\varepsilon_3}\times\frac{A_e}{A_3} \quad (18)$$

A_e, area of the upper surface of the element is equal to $\Delta x\Delta y$. Area A_3, temperature T_3, and emission coefficient ε_3 are related to bottom surface of the thermal shield. Also, $F_{e\text{-}up\infty}$ is element configuration factor to upper environment. In order to solve the problem, equation (17) must be solved simultaneously with the three equations (19), (20), and (21) in a manner that values of energy rates will be the same in these equations.

$$\dot{q}_{rad-slab\to tun}=\sum_j\sum_i\frac{\sigma(T_{ij}^4-T_3^4)}{R_{ij}}\Delta x\Delta y \quad (19)$$

$$\dot{q}_{cond-tun}=k_{tun}\frac{(T_3-T_4)}{THK_{tun}}A_3 \quad (20)$$

$$\dot{q}_{rad\,\&\,conv-tun}=[h_4(T_4-T_{up})+\sigma\varepsilon_4(T_4^4-T_{up\infty}^4)]\Delta x\Delta y \quad (21)$$

$\dot{q}_{rad-slab\to tun}$ is sum of radiation energy rates from all elements of the strip reaching the shield, $\dot{q}_{cond-tun}$ is conductive energy rate passing through the shield, $\dot{q}_{rad\,\&\,conv-tun}$ is radiative and conductive energy rate emitted from top of the shield. K_{tun}, and THK_{tun}, are thermal conductivity, and thickness of shield. Also, ε_4, and T_4 are emissivity factor and temperature of bottom surface of shield.

In the case that heat sources are presented at bottom surface of the shield, temperature of gas between the shield and strip can be controlled by combustion process. Energy balance for an element in this situation will be like the following form:

$$\frac{\partial T}{\partial t}=\frac{k}{\rho c}\left(\frac{\partial^2 T}{\partial x^2}+\frac{\partial^2 T}{\partial y^2}\right)-\frac{1}{\rho c\Delta z}\left[h_{up}(T-T_g)+h_{down}(T-T_{down})\right]-\frac{\dot{q}_{rad-e\to tun}}{\rho c\Delta z} \quad (22)$$
$$-\frac{\sigma\varepsilon}{\rho c\Delta z}\left[F_{e-roll}(T^4-T_{roll}^4)+F_{e-down}(T^4-T_{down\infty}^4)+F_{e-up\infty}(T^4-T_{up\infty}^4)\right]$$

Where T_g is the temperature of gas inside of the shield, and $\dot{q}_{rad-e\to tun}$ is thermal energy rate which is released from top surface of the element to the shield through radiation. Sum of radiative energy rates from all elements of the strip and the gas reaching the shield can be computed from the following relation:

$$\dot{q}_{rad-slab\,\&\,g\to tun}=\sum_j\sum_i\dot{q}_{rad-e\,\&\,g\to tun} \quad (23)$$

In relations (22) and (23), an equivalent radiation circuit has been assumed among an arbitrary element, gas, and the shield in order to compute $\dot{q}_{rad-e\,\&\,g\to tun}$, input thermal energy rate into the bottom surface of shield from the element surface due to the presence of the gas, and $\dot{q}_{rad-e\to tun}$. The equivalent electric circuit was used to compute these values simultaneously.

Equations (16), (17), and (22) are parabolic and can be stated in the following general form:

$$\frac{\partial T}{\partial t}=\frac{k}{\rho c}\left(\frac{\partial^2 T}{\partial x^2}+\frac{\partial^2 T}{\partial y^2}\right)+S \quad (24)$$

An explicit method has been used in solution. The forward difference derivative approximation was used for thermal derivative term and the central difference derivative approximation was used for spatial derivative term. When equation is discrete, temperature in new time step is computed as below using the data in the preceding time step.

$$T_P^{n+1}=T_P^n+\frac{k\Delta t}{\rho c}\left(\frac{T_E^n-2T_P^n+T_w^n}{\Delta x^2}+\frac{T_N^n-2T_P^n+T_S^n}{\Delta y^2}\right)+S^n\Delta t \quad (25)$$

Where T_P is temperature of an element for which energy balance is written. T_N, T_S, T_E, and T_W are temperatures of the elements located above, below, right and left of the considered element. S^n is a constant source term which is calculated at previous time step. The accuracy of the solution is of the first order in time and second order in space. Convergence condition of above equation will occur when:

$$\frac{k\Delta t}{\rho c}\left(\frac{1}{\Delta x^2}+\frac{1}{\Delta y^2}\right)\le\frac{1}{4} \quad (26)$$

Results and discussion

A computer code was developed to solve the equations. Accuracy of the code was checked by temperature measurement of the strip at MSC. Two points of the strip temperature, first and end of the strip, were measured and checked with the results of the computer code. Good agreements were shown for these measured and calculated temperatures. Values are shown in Figures (1-b) and (1-d).

Temperature distribution along the strip for mesh sizes of 750×20, 1500×40, and 3750×100 has been calculated. Because the results for 2 last finer meshes have good agreement, the graphs for the mesh size 3750×100 are presented here.

Temperature contours are presented in Kelvin over half of the strip for different time periods and three different cases, with thermal shield, without thermal shield, and with both thermal shield and heat source in Figures (1), (2), and (3). Horizontal and vertical axes represent length and width of the strip, respectively. In all of these figures only the part of strip which is moving over the transfer table is shown and the part of slabs under rolling shelves isn't

shown.

Figure (1) shows temperature reduction over half of the strip in different times when the strip is passing through the transfer table without thermal shield. From this Figure, temperature drop at middle sections near front edge of the strip and at the time of entering the first finishing stand, F1, is around 100 K (Figure1-b), but near end edge of the strip at the time of entering finishing shelves is about 200 K (Figure 1-d). This difference indicates uneven temperature distribution within the strip when entering F1. Another considerable point is the creation of high temperature gradient and a rapid temperature reduction at the edges. This gradient is due to the high amount of radiative heat transfer at the strip edges.

In the situation with thermal shield, temperature reduction in half of the strip is shown in Figure (2) for different times of passing through the transfer table. It is seen that temperature reduction for the middle sections near front edge of the strip is around 40 K at the time of entering F1 (Figure 2-b), which shows a reduction of 60 K as compared to the previous situation. Temperature reduction near end edge of the strip is about 130 K at the time of entering F1 (Figure 2-d), which shows a reduction of 70 K compared to the previous section. A considerable point in this figure is the reduction in gradient and temperature reduction at the strip edges.

In the case where heat source (combustion) is used in addition to the thermal shield, a more even temperature distribution is observed, Figure (3) depicts this subject. Temperature reduction for middle sections near front edge and at the time of entering F1 shelf reaches approximately 37 K (Fig.3-b), which shows a reduction of 3 K compared to the previous case. Temperature reduction near end edge is around 150 K at the time of entering F1 (Figure 3-d). This is a reduction of 25° K compared to the previous case.

The heat transfer from surface of the strip has also been computed in this study for all cases. Figure (4) depicts heat transfer in the case that there isn't thermal shield over transfer table. The continuous line represents heat loss from the whole strip surface and the broken line represents heat loss by radiation from top surface of the strip at each moment. As the strip exits from last shelf of roughing around the 20th second, a larger surface of the strip is exposed to the environment at each moment and, consequently, heat loss in the strip surface will be greater at each moment. From this moment on, and given that whole surface of the strip has been exposed to air, heat loss at each moment will be reduced as a result of reduction in strip temperature. From the 30th second on, speed of strip is reduced because the strip enters finishing stand, which leads to a reduction in convective heat transfer rate. Also surface of the strip which is exposed to ambient continues to reduce which leads to a reduction in radiation heat transfer rate, consequently, heat loss from surface of strip reduces and at the end becomes zero when whole of the strip enters finishing stand. The total heat loss for the strip after passing through transfer table is equal to 1.74 Mega Joules.

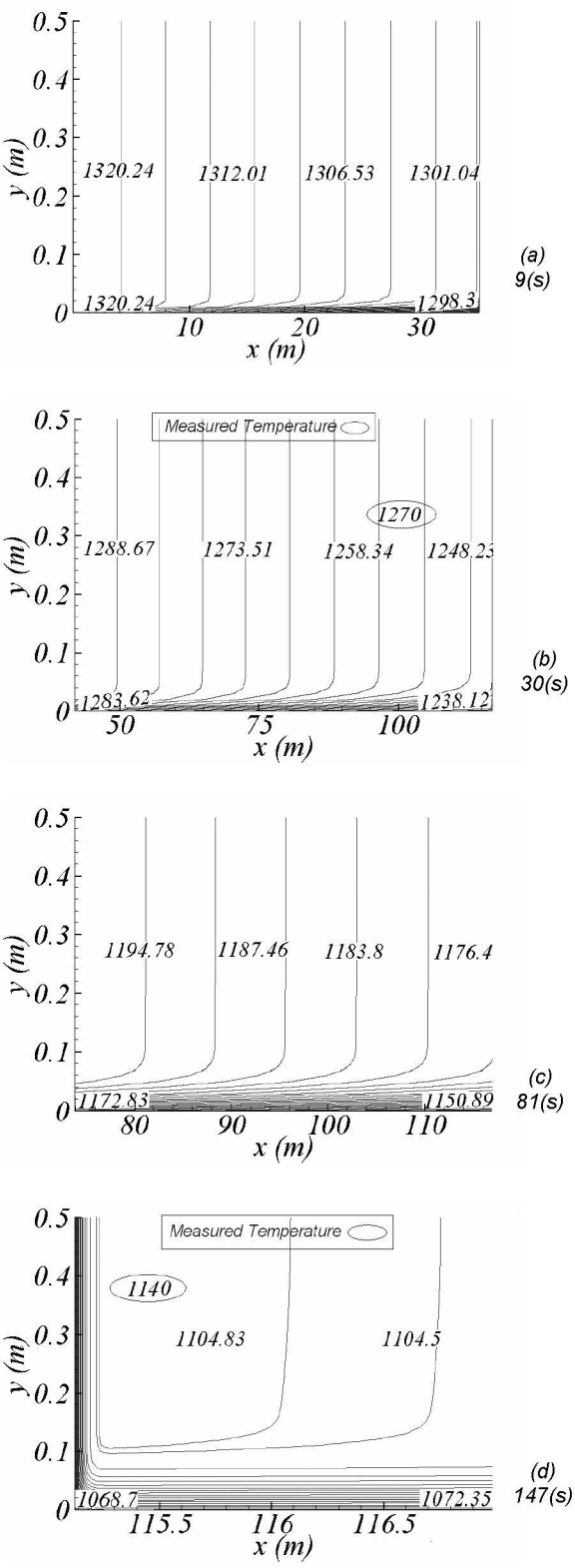

Fig. 1 Temperature counters at different times without thermal shield.

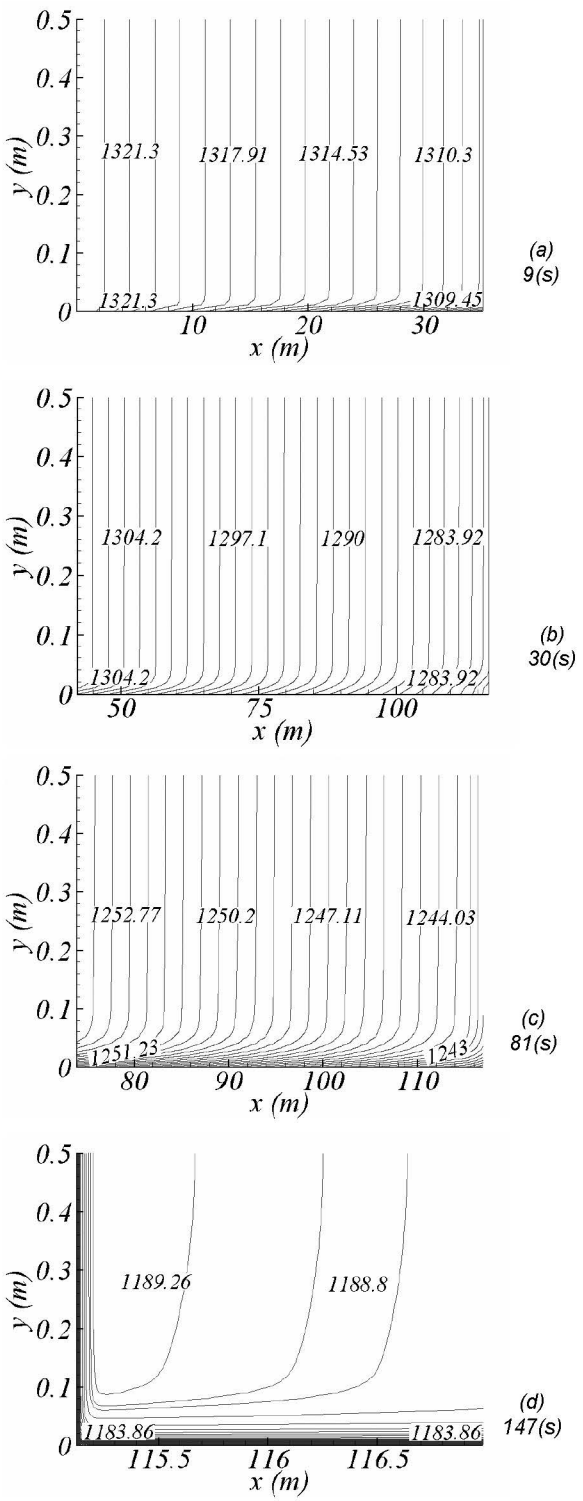

Fig. 2 Temperature counters at different times with thermal shield.

Figure (5) shows heat transfer when thermal shield is used. The continuous line represents heat loss from the whole strip surface and the broken line represents radiative heat loss from the top of the strip at each moment. The noteworthy point at this stage is high reduction in heat loss from top surface of the strip. This reduction is due to presence of the thermal shield over top surface and also because of reduction in radiation rate from top surface. As a result of reduction in heat loss, the overall heat loss also reduces considerably. The total heat loss after passing through transfer table is 0.98 Mega Joules, which shows a reduction of 45% as compared to the previous case.

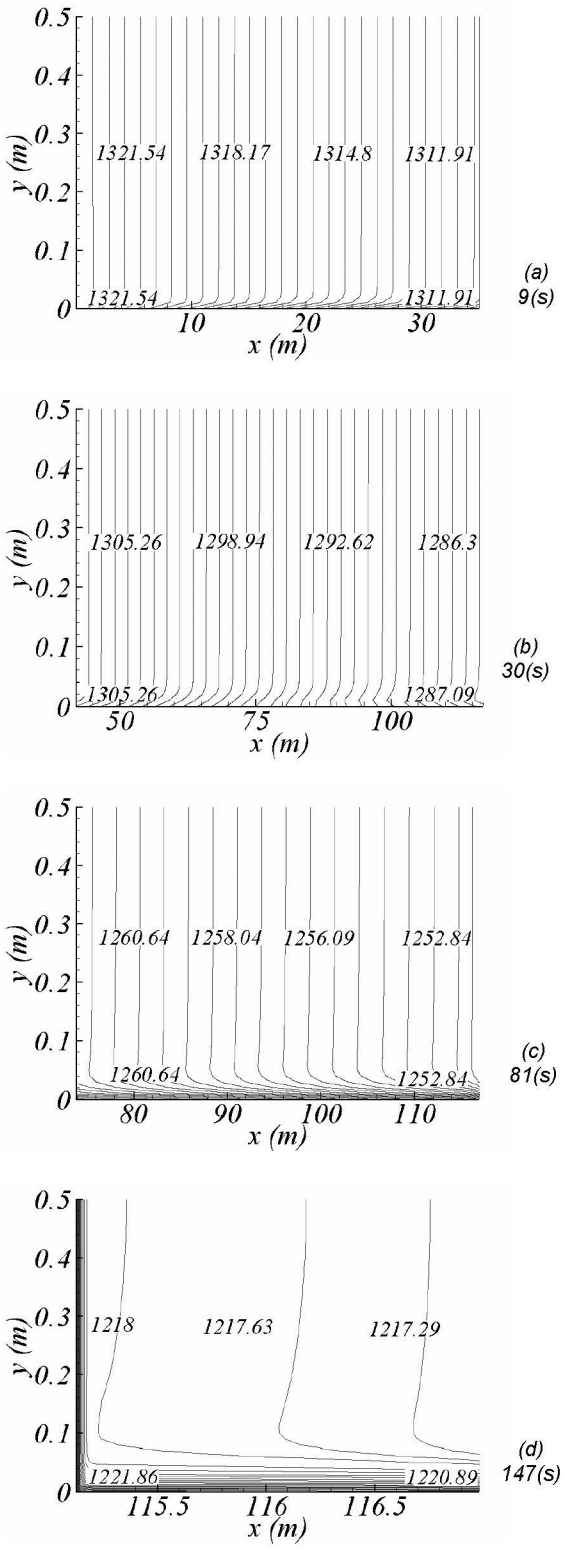

Fig. 3. Temperature counters at different times with thermal shield and heat source.

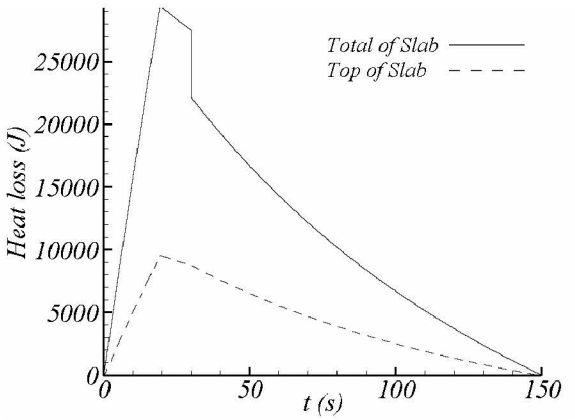

Fig. 4. Heat loss of top and whole surfaces of slab without thermal shield.

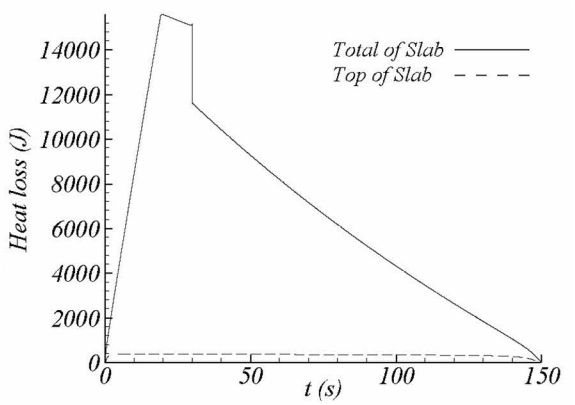

Fig. 5. Heat loss of top and whole surfaces of slab with thermal shield.

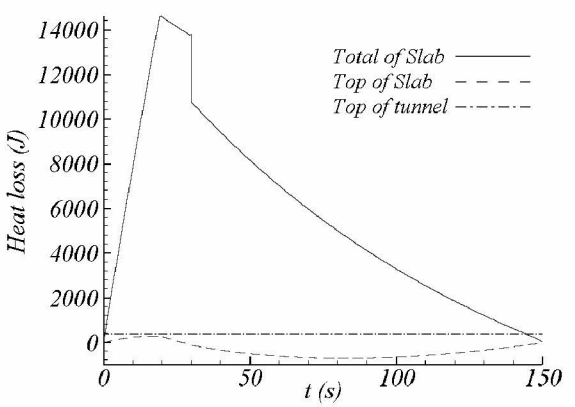

Fig. 6. Heat loss of top and whole surfaces of slab with thermal shield and heat source.

Figure (6) depicts heat transfer in the case where thermal shield and heat source are used. Here, the total heat loss from the strip after passing through transfer table is 0.84 Mega Joules, which is around 10% lower than the case with only thermal shield. The point to note here is the absorption of heat from top surface and edges of the strip from around the 30th second on. Energy absorption occurs when strip temperature falls below gas temperature. Energy is absorbed in this case through radiation and convection. This state of affairs is due to the presence of the shield above the strip and also to the presence of high temperature gas inside the shield.

Conclusions

The following results were obtained from the simulation of heat transfer in a strip passing through the hot rolling mill at Mobarakeh Steel Complex (MSC) under three different caces: without thermal shield, with thermal shield, and with both thermal shield and heat source:

1- Temperature distribution was estimated for all three cases.

2- Heat transfer from the strip surface was computed.

3- Compared to the case without thermal shield, temperature distribution was more even and a reduction of 45% in heat transfer from the surface was observed in the case when a thermal shield is used.

4- Compared to the case with thermal shield only, more even temperature distribution was observed in the case with both thermal shield and heat source. Heat loss in this case was 10% less than the case with only thermal shield.

5- From the results obtained, it may be claimed that use of the thermal shield is associated with such benefits like reduction in temperature difference along the slab, reduction in material losses, production costs, and energy consumption.

References

[1] V. B. Ginzburg, Iron and Steel Eng., (1985), 21.
[2] V. B. Ginzburg, W. F. Schniedburg, Iron and Steel Eng., (1986), 29.
[3] S. Serajzadeh, A. Karimi Taheri, F. Mucciardi, Model. Simul. Mater. Sci. Eng., 10 (2002), 185.
[4] S. Serajzadeh, A. Karimi Taheri, F. Mucciardi, Int. J. Mech Sci. 44 (2002), 2447.
[5] S. Serajzadeh, A. Karimi Taheri, Model. Simul. Mater. Sci. Eng. 11 (2003), 179.
[6] S. Serajzadeh, App. Math. Model., article in press, (2003).
[7] H. B. H. Khadem, Msc. Thesis, Dept. of Mech., Isfahan University of Technology, (1998).
[8] F. P. Incropra, D. P. Dewit, 2nd Vol., 2nd Ed., (1990).
[9] N. Ramachandran, B. F. Armaly, T. S. Chen, ASME J. Heat Transfer,109 (1987), 1036.
[10] W. M. Kays, M. E. Crawford, Convective heat and mass transfer, Second Edition, McGraw-Hill, New York, (1980).
[11] T. Fuji, H. Imura, Int. J. of Heat and Mass Transfer, 15 (1972), 755.
[12] Y. Hayashi, A. Takimoto, K. Hori, 14th Japan heat transfer symp., (1977), 4.
[13] http://www.me.utexas.edu/~howell/.
[14] J. P. Holman, Heat transfer, Eighth Edition, McGraw-Hill, New York, (1997).